

Physical properties of Martian meteorites: Porosity and density measurements

Ian M. COULSON^{1,2*}, Martin BEECH³, and Wenshuang NIE³

¹Solid Earth Studies Laboratory (SESL), Department of Geology, University of Regina, Regina, Saskatchewan S4S 0A2, Canada

²Institut für Geowissenschaften, Universität Tübingen, 72074 Tübingen, Germany

³Campion College, University of Regina, Regina, Saskatchewan S4S 0A2, Canada

*Corresponding author. E-mail: ian.coulson@uregina.ca

(Received 11 September 2006; revision accepted 06 June 2007)

Abstract—Martian meteorites are fragments of the Martian crust. These samples represent igneous rocks, much like basalt. As such, many laboratory techniques designed for the study of Earth materials have been applied to these meteorites. Despite numerous studies of Martian meteorites, little data exists on their basic structural characteristics, such as porosity or density, information that is important in interpreting their origin, shock modification, and cosmic ray exposure history. Analysis of these meteorites provides both insight into the various lithologies present as well as the impact history of the planet's surface. We present new data relating to the physical characteristics of twelve Martian meteorites. Porosity was determined via a combination of scanning electron microscope (SEM) imagery/image analysis and helium pycnometry, coupled with a modified Archimedean method for bulk density measurements. Our results show a range in porosity and density values and that porosity tends to increase toward the edge of the sample. Preliminary interpretation of the data demonstrates good agreement between porosity measured at 100× and 300× magnification for the shergottite group, while others exhibit more variability. In comparison with the limited existing data for Martian meteorites we find fairly good agreement, although our porosity values typically lie at the low end of published values. Surprisingly, despite the increased data set, there is little by way of correlation between either porosity or density with parameters such as shock effect or terrestrial residency. Further data collection on additional meteorite samples is required before more definitive statements can be made concerning the validity of these observations.

INTRODUCTION

Much attention is presently being directed toward the study of the planet Mars. Numerous robotic and in-orbit reconnaissance missions are currently being planned and/or executed; future missions call for the extraction and return to Earth of Martian surface material. Martian meteorites are now accepted to be fragments of the Martian crust (e.g., McSween 1994; Clayton and Mayeda 1996); for the time being, they represent the only samples of Mars that are available for analysis on Earth. While the current NASA Mars Exploration Rovers provide unrivaled, albeit limited, observational and chemical data in situ, relating to surface soils and rock types (e.g., Squyres et al. 2004; Herkenhoff et al. 2004), Martian meteorite samples provide further insight into the various lithologies present, and also a history of distinct ancient impacts on the surface and/or near-surface of Mars (Head et al. 2002; Eugster et al. 2002). Comprehensive study of these meteorites may also aid in defining the needs for future

Mars missions and, in particular, the requirements for sample return (Meyer 2006).

While the chemical make-up and petrology of the 36 currently known Martian meteorites have been studied extensively (e.g., McSween and Treiman 1998; Bridges et al. 2001; Lin et al. 2005), relatively little data exists on their basic structural characteristics, such as porosity or density (cf. Flynn 2004; Beech and Coulson 2005; Consolmagno et al. 2006). A recent survey revealed, for example, that only eight fragments from four distinct Martian meteorites have measured and published porosity values (Britt and Consolmagno 2003). Porosity is of fundamental importance since it is a measure of the volume of empty space within a meteorite; it also offers clues to their nature and evolution (Yomogida and Matsui 1983; Consolmagno et al. 1998). Indeed, to fully interpret the origin, shock modification, and cosmic ray exposure history of a meteorite, some measure of its porosity must be known. Here we report on the results of a program recently begun to measure the physical

characteristics, specifically porosity and density, of Martian meteorites. These properties were determined via a combination of scanning electron microscope (SEM) imagery/image analysis of thin section samples and helium pycnometry, coupled with a modified Archimedean method for bulk density measurements of macroscopic fragments of the meteorites. Twelve Martian meteorites (represented by 16 samples) are examined in this study; these include representatives of all the currently recognized meteorite groups (see Tables 1–3 for a detailed sample listing).

METHODOLOGY

Physical properties of the Martian meteorites were determined in a number of distinct ways. First, porosity was measured through electron microscopy and image analysis of the samples, a method that has been successfully applied and evaluated by Straight, Britt, and Consolmagno in their studies of terrestrial and meteoritic samples (Straight and Consolmagno 2001, 2002, 2003; Britt and Consolmagno 2003). Specifically the porosity (ϕ), which is a measure of empty space inside a rock, was determined by imaging polished thin sections (30 μm thick) of each individual meteorite using an SEM. Serial backscattered electron (BSE) images were collected throughout at fixed magnifications of 100 \times and 300 \times (Fig. 1). ϕ was determined as the percentage ratio of the summed void area divided by the total area of the image. Standard image analysis software was applied to each image in turn to determine the percentage of void space, which represents both connected and unconnected porosity (see below). Hence, this method of analysis determines the “total porosity” (ϕ). The Jeol JSM-6360 SEM used in this study is located in the Department of Geology, University of Regina. An Oxford Instruments energy dispersive spectrometer (EDS) was fitted to this instrument, facilitating phase identity within the samples. Typical operating conditions were 10 kV beam current and a relative spot size of 70; images were collected at the slowest scan rate and at a resolution of 1280 \times 960 pixels. Soft Imaging Systems GmbH, “analysis” image analysis software was employed for image processing. For the sake of brevity, this method is hereafter referred to as SEM/IA.

The void area was calculated on an image-by-image basis for a given meteorite, with minimal overlap (nominally 5%) between frames. This was performed to minimize potential biased contributions to the void estimate from overlap areas. Those images that contained a portion of the natural surface of the thin section within their area were denoted “edge,” while the remainder are collectively termed “center” images. The method of void-space identity during image analysis was employed in a similar manner to that described in detail by Corrigan et al. (1997), in that images were imported at their original resolution into the image analysis software program. The software supports images in

256-level grayscale, and through application of its user-adjustable threshold utility, an optimal value was chosen to distinguish void-space. It was necessary to adjust this value to different levels for the various meteorite samples studied (e.g., differences relating to slight changes in background brightness or contrast levels during image acquisition). However, provided that all images for a single meteorite were collected in one analytical session, a fixed value of grayscale could be used throughout for each image-processing run. Optimal threshold selection was attained using the software’s histogram function, with peaks corresponding to mineral grains and low levels of grayscale to void-space. The software facilitated this step with the use of color-coding for each “peak,” or grayscale range on the histogram—a feature that allowed rapid and easy determination of the modal mineralogy (and void area) present. This latter calculation is based on the percentage of selected pixel area to overall image area. EDS was employed during image collection to confirm the absence of material in areas thought to represent void-space (i.e., no alteration products present). The spatial resolution of this method is better than 1 micron for images of 100 \times or 300 \times ; as such, 4 orders of magnitude in terms of void size can be measured in this way (about a centimeter down to the micron scale).

Despite the successful application of SEM/IA in meteorite porosity studies, the method is not without problems. Recent studies (Straight and Consolmagno 2004, 2005) demonstrate that caution must be used in interpreting data obtained in this way. For example, it is important to try and recognize and eliminate the potential effects of sample preparation on porosity (i.e., cracks induced during making of a thin section). A good indicator in the case of microcrack porosity is whether these were present prior to the making of the thin section. If weathering material(s) are present within such fractures (Fig. 2), it would seem likely that they are not then the result of sample preparation “damage.” Straight and Consolmagno (2004, 2005) provide a more critical assessment of errors for SEM/IA, but note that it is very difficult to assess the uncertainty of this method. However, in keeping with the findings of Corrigan et al. (1997), we are confident that our analytical methodology yields accurate porosity measurements. The authors can provide interested readers with the individual porosity calculation data resulting from the image processing.

In an attempt to assess any potential difficulties with our own results, a second method of determining ϕ , which employed helium pycnometry (a technique based on the ideal gas law), was completed where macroscopic samples of meteorite were available. Here ϕ is calculated from replicate measurements of volume and density (see Rust et al. 1999 for details):

$$\text{porosity } \phi = (1 - \rho_b/\rho_g) \times 100 \quad (1)$$

where ρ_b is the bulk density and ρ_g is the grain density.

Table 1. Summary of Martian meteorite porosity (ϕ) determined via SEM/IA.

Type of meteorite	No. of images	100×			No. of images	300×			Comments
		Center	Edge	Total		Center	Edge	Total	
Orthopyroxenite class									
Allan Hills (ALH) 84001,86	60	3.63	3.81	3.69	60	0.90	2.52	1.66	
Dunitite class (chassignite)									*Average value for the 2 grains
Chassigny BM1985.M173 (grain 1)	43	5.83	5.14	5.55	100*	7.82	9.00	8.41	
Chassigny BM1985.M173 (grain 2)	42	3.19	3.94	3.49					
Shergottite class									
Dar al Gani 476	53	1.86	2.34	2.27	344	2.62	3.58	2.77	Olivine-orthopyroxene shergottite
Elephant Moraine (EET) A79001,90 (Lith. A)	82	10.46	11.74	11.04	580	10.51	9.84	10.41	Olivine-phyric shergottite
Northwest Africa (NWA) 3171	389	6.13	7.71	6.61	30	9.14	9.76	9.20	Basaltic shergottite
Queen Alexandra Range (QUE) 94201,4	88	2.18	6.92	3.52	100	3.38	2.33	2.86	Basaltic shergottite
Zagami BM1966,54	155	1.43	3.59	1.94	100	1.79	3.12	2.46	Basaltic shergottite
ALHA77005,54	203	4.86	5.55	5.01	100	6.19	5.76	5.98	Lherzolitic shergottite
Lewis Cliff (LEW) 88516,18	62	8.40	3.99	6.74	100	8.24	4.84	6.54	Lherzolitic shergottite
Clinopyroxenite class (nakhlites)									
Miller Range (MIL) 03346, 131	78	2.47	3.34	2.97	100	3.03	4.17	3.60	
MIL 03346, 170	160	4.90	3.17	4.48	100	3.39	3.41	3.40	
Nakhla BM1913,26 (P7017)	35	2.98	4.61	3.72	100	3.12	4.47	3.80	
Nakhla P7635	64	1.50	3.18	1.92	100	6.61	8.51	7.56	
Basalt (Mt. Etna) IC2003-01	540	11.55	13.12	11.72					Earth analogue (shergottite)

Table 2. Sample areas (mm²) measured during SEM/IA porosity determinations.

Meteorite		100×		300×	
		Porosity area	Total area	Porosity area	Total area
ALH 84001	Edge	7884	206,937	8156	323,629
	Center	14,276	393,216	3334	368,640
	Total	22,161	600,153	11,490	692,269
Chassigny (Grain 1)	Edge	8378	163,102	–	–
	Center	14,331	245,760	–	–
	Total	22,710	408,862	–	–
Average for both grains					
(Grain 2)	Edge	6983	177,229	55,299	614,400
	Center	8225	258,048	4,8053	614,400
	Total	15,208	435,277	103,352	1,228,800
Dar al Gani 476	Edge	36,331	1,554,052	18,697	521,869
	Center	5018	270,336	74,187	2,826,240
	Total	41,349	1,824,388	92,883	3,348,109
EETA79001 (Lith. A)	Edge	39,959	340,307	96,705	982,892
	Center	43,701	417,792	577,431	5,492,736
	Total	83,660	758,099	674,137	6,475,628
NWA 3171	Edge	95,582	1,240,381	3598	36,864
	Center	174,911	2,853,847	27,924	305,630
	Total	270,492	4,094,228	31,522	342,494
QUE 94201	Edge	13,103	189,243	14,293	614,400
	Center	10,459	479,232	20,771	614,400
	Total	23,562	668,475	35,064	1,228,800
Zagami	Edge	11,747	327,455	19,178	614,400
	Center	15,154	1,056,768	11,023	614,400
	Total	26,901	1,384,223	30,201	1,228,800
ALHA77005	Edge	20,568	370,390	35,361	614,400
	Center	66,247	1,363,968	38,009	614,400
	Total	86,815	1,734,358	73,370	1,228,800
LEW 88516	Edge	6510	163,115	28,742	614,400
	Center	22,714	270,336	59,645	614,400
	Total	29,224	433,451	88,387	1,228,800
MIL 03346, 131	Edge	8836	264,228	25,609	614,400
	Center	4861	196,608	18,590	614,400
	Total	13,697	460,836	44,199	1,228,800
MIL 03346, 170	Edge	8568	270,163	20,943	614,400
	Center	41,562	847,872	20,838	614,400
	Total	50,130	1,118,035	41,781	1,228,800
Nakhla (BM1913)	Edge	7057	153,092	27,485	614,400
	Center	5491	184,320	19,178	614,400
	Total	12,548	337,412	46,663	1,228,800
Nakhla (P7635)	Edge	5352	168,155	52,275	614,400
	Center	7562	503,808	40,606	614,400
	Total	12,914	671,963	92,881	1,228,800
Basalt (Mt. Etna)	Edge	87,872	669,965	–	–
	Center	628,520	5,443,584	–	–
	Total	716,392	6,113,549	–	–

Table 3. Summary of density and porosity determinations via He pycnometry.

Type of meteorite	Bulk density	St. dev. (1σ)	Grain density	St. dev. (1σ)	Porosity	Comments
Olivine-phyric shergottite	3.29	0.05				Sayh al Uhaymir 005
Olivine-orthopyroxene shergottite			3.13	0.02		Dar al Gani 489
Basaltic shergottite			3.42	0.2		Zagami
Clinopyroxenite			3.56	0.2		Nakhla
Dunite	3.46	0.02	3.69	0.02	6.23	Chassigny

Bulk and grain densities are the mean of 5 replicate analyses.

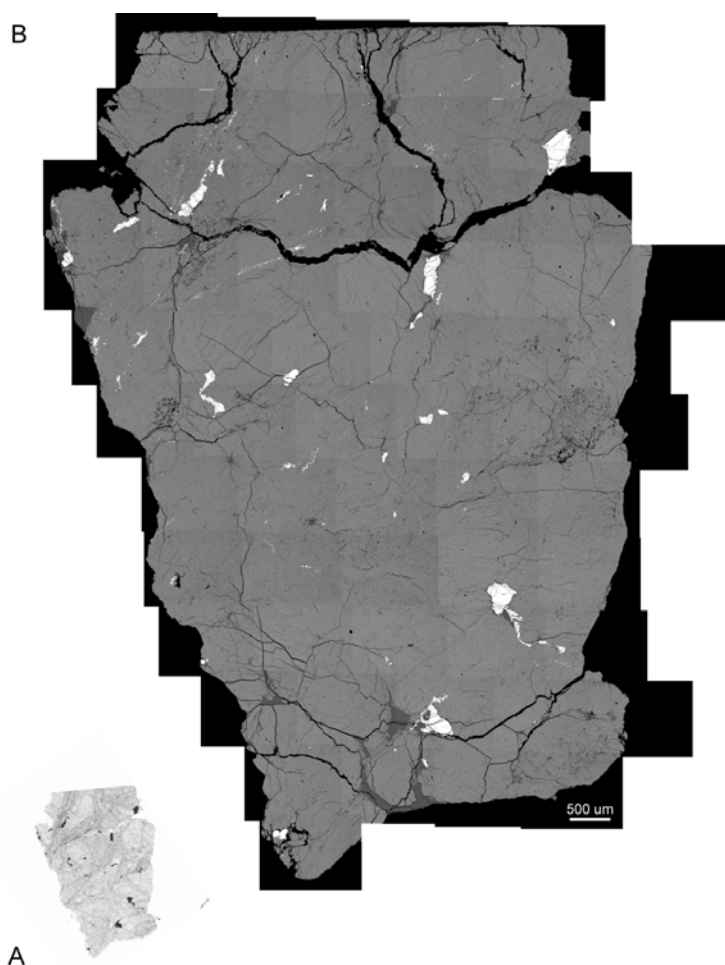


Fig. 1. a) Thin section of Martian orthopyroxenite meteorite sample ALH 84001,86 taken under plane-polarized light. Dimensions are approximately 6×10 mm. b) Composite BSE image collected for the same specimen. Scale bar represents 500 microns. Individual images were collected at $100\times$ magnification.

The helium pycnometer utilized in this study was manufactured by Micromeritics (AccuPyc 1330 model) and housed in the Centre for Experimental Study of the Lithosphere (CESL), Department of Earth and Ocean Sciences, University of British Columbia, Canada.

The density measurements presented in this study are based on the modified Archimedean method of Consolmagno and Britt (1998) with glass beads substituting for liquid. This method was favored as it is non-contaminating to the meteorites on loan. This procedure has been evaluated by Wilkison and Robinson (1999, 2000a, 2000b), who made repeated measurements of meteorite samples using 250–425 μm size glass beads, and showed that this technique was both reliable and accurate. In their studies they were able to match the densities measured on standard meteorite samples to within 1% and a precision better than 2.1%. We have also analyzed a range of common meteorite types (e.g., Gao and Sikhote-Alin) in this way to verify the copacetic operation of this technique.

This second method potentially underestimates the ϕ of the meteorite; if there are unconnected pores not accessed by the helium, the volume of the sample is overestimated as it includes the unconnected pore volume. Therefore, this method yields only the “connected porosity.” The connected porosity is equal to the total porosity (ϕ) only if all pores are connected (Rust et al. 1999). As has been noted by others, unconnected pore volume is a particular problem for basaltic igneous rocks, ergo, it is important to try and quantify this in any study of the Martian achondritic meteorites.

One final point is that both the He pycnometry and the bulk sample density measurement techniques begin to fail at smaller sample masses (<20 g) as errors related to reproducibility and precision begin to increase (McCausland and Flemming 2006). Wilkison et al. (2003) discuss in some detail this type of error assessment, and as such it is advisable to judge both bulk and grain densities accordingly.

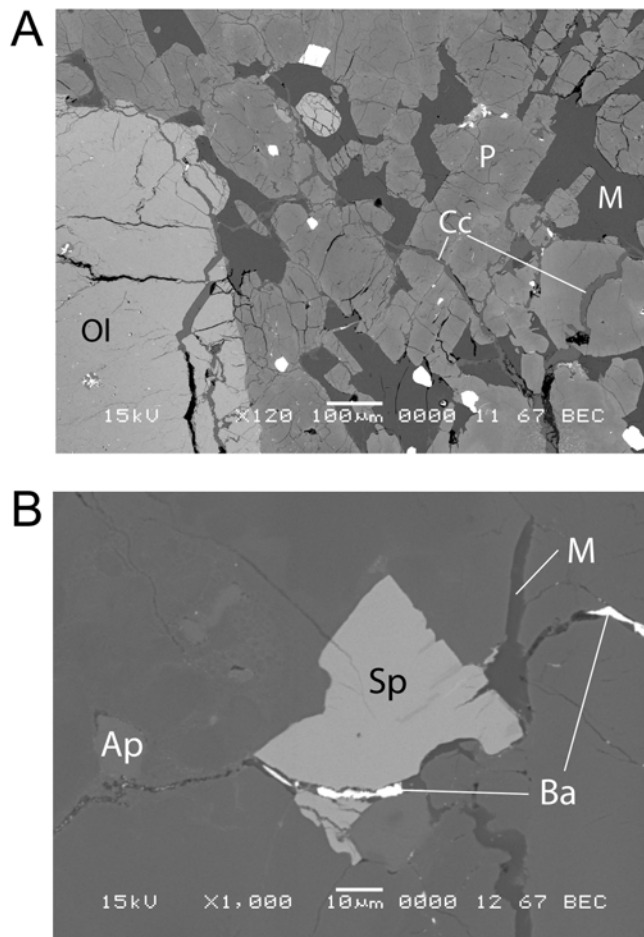


Fig. 2. BSE images of alteration products: calcite (Cc) and baryte (Ba) infilling cracks/fractures within the olivine-orthopyroxene-phyric shergottite Dar al Gani 476. Image (a) taken at 120 \times magnification and (b) taken at 1000 \times magnification. Other phases are olivine (Ol), maskelynite (M), pyroxene (P), apatite (Ap), and spinel (Sp).

Sample Selection

The aim of this study was to explore and characterize the physical properties of Martian meteorites. As these meteorites have been subdivided into a number of groupings, we thought it prudent to select for study representatives from each different group. This has the added benefit of facilitating comparison between individuals and group members. In short, Martian meteorites are igneous rocks with a range of terrestrial basaltic and ultramafic mineral assemblages that have experienced various degrees shock and alteration (Bridges and Warren 2006). At the present time, they are categorized as shergottites, clinopyroxenites (nakhlites), dunites (chassignites), and a single orthopyroxenite. The shergottites are further divided into basaltic, lherzolitic, olivine-phyric, and olivine-orthopyroxene-phyric types, relating to mineral abundances and inferred origins (e.g., Goodrich 2002). As such, our study includes representative

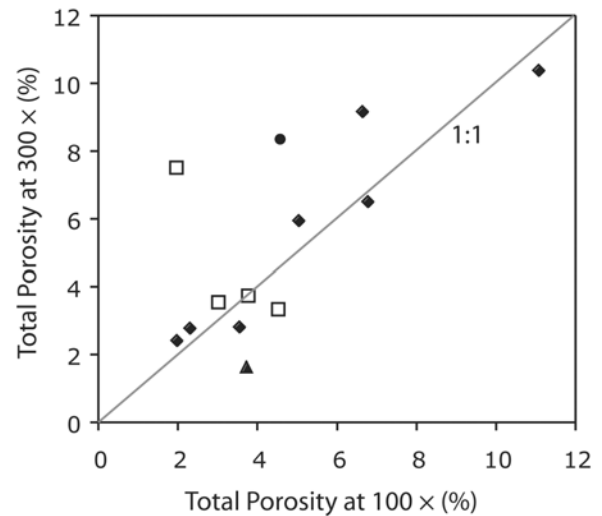


Fig. 3. Comparison of total porosity ϕ (%) at 100 \times and 300 \times magnification for Martian meteorite samples, as determined in this study. The porosity data derive from Table 1. Multiple data points are for clinopyroxenites (squares), dunites (filled circle), orthopyroxenite (filled triangle), and shergottites (filled diamonds). Note, however, that the data for dunite is an average value for the two fragments.

Martian meteorites from the following categories: orthopyroxenite (1), dunite (1), clinopyroxenite (2), basaltic shergottite (3), lherzolitic shergottite (2), olivine-phyric shergottite (2), and olivine-orthopyroxene-phyric shergottite (1) (see Tables 1–3 for details). As a potential analogue to the shergottites, we included for analysis a sample of basalt from the 2002–03 eruptions of Mount Etna, Italy.

RESULTS

Measured values of porosity ϕ and density (ρ_b and ρ_g) are listed in Tables 1 and 3 and shown in Figs. 3–6. The results, presented as part of this study, show that there is quite a range in porosity and density values for all the samples studied, and that these closely agree with those few published data in the literature. Some of the meteorites also approach but do not exceed those values for the studied basalt from Mt. Etna (~12%), this being a good measure of having resulted from initial crystallization and vesiculation during rapid cooling upon eruption. The porosities corresponding to the sample edges and interior have been measured and evaluated separately. Consistent with the studies by Consolmagno et al. (1998) and Strait and Consolmagno (2001, 2002), we find that porosity tends to increase toward the edges of the sample on the thin section (Fig. 1), where larger cracks are certainly more evident. However, it was also noted that many of the fractures are infilled with secondary minerals (Fig. 2), related in part to the chemical alteration and weathering of the meteorite (Crozzaz and Wadhwa 2001). Figure 3 is a plot comparing the

variation between measured porosity (ϕ) at 100 \times and 300 \times magnification. Our initial justification for doing this was to evaluate whether there was an underestimation of the porosity at 100 \times magnification—for example, the presence of micron-sized pore space not discernible at this magnification (Fig. 4). Although there is a good correlation between the data and thus we can be confident that measurement of porosity at 100 \times magnification is a suitable starting point, some anomalies are evident. For example, the Martian meteorite samples that represent cumulate rocks can have either a raised or lowered ϕ at higher magnification. In the case of orthopyroxenite, this is most likely to be explained as the result of sample inhomogeneity on the microscopic scale, particularly as for this sample we only obtained a small subset of images at higher magnification (Tables 1 and 2). Furthermore, although the shergottites show the most consistent porosities regardless of magnification by far, this is not universal, and one of the lherzolitic shergottites shows a lower porosity at the higher magnification. In view of our original thoughts concerning underestimation of porosity at lower magnification, this would seem an unlikely scenario. Although this could again reflect inhomogeneity on the scale of the studied thin section perhaps, in this case, the porosity variation relates to the presence of abundant areas of glass induced by shock melting within this particular meteorite (Mikouchi et al. 1998). The significance of the trends exhibited by ϕ in relation to other factors is discussed in detail in the following section.

DISCUSSION

It is well known that several distinct types of porosity can be distinguished. First, a distinction should be drawn between connected and non-connected porosity. In addition, the “empty space” regions that the porosity describes can be due to cracks, vugs, and/or gaps between distinct mineral grains and assemblages. The most common type of porosity observed within meteorites, however, is that due to cracks that may be either connected or non-connected. While the former can be measured by the standard He pycnometer technique, the latter can not. SEM/IA, however, has in principle the advantage of being able to measure both, but may face additional problems, such as damage caused during sample preparation or porosity that is inhomogeneous on the scale of a thin section (Straight and Consolmagno 2004).

Not only is the overall porosity the sum of several distinct forms, it will also vary according to the meteorite’s crystallization and compaction history (which determines primary porosity), its collisional history, and its terrestrial residency time. In the final case, for example, one might expect the porosity to decrease with time due to the growth of secondary minerals within the pore space. Such weathering effects will vary according to whether the meteorite fell in a

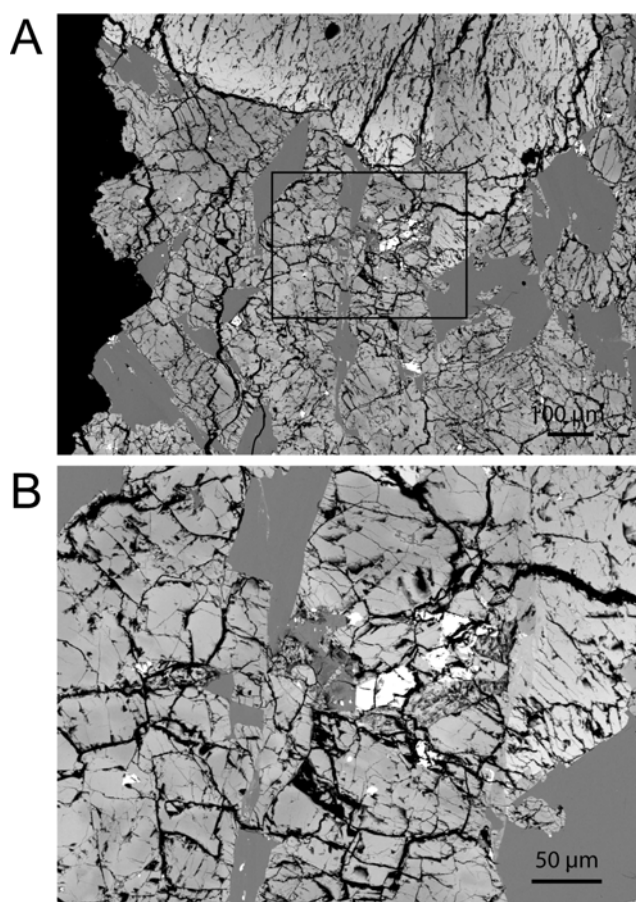


Fig. 4. Comparison of BSE images collected at a) 100 \times and b) 300 \times magnification of the olivine-phyric shergottite EETA79001 (lith. A). Area in (b) coincides with an area close to the center of (a) and is highlighted. The higher magnification image clearly shows more detail in terms of microfractures and porosity.

cold or hot desert or a temperate region. The Dhofar 019 shergottite found in the hot desert of Oman, for example, contains secondary calcite (present mainly as cross-cutting veins), gypsum, smectite, celestite, and Fe hydroxides (Taylor et al. 2002). Indeed, Crozaz and Wadhwa (2001) note that for those meteorites found in hot deserts, fractures are often observed to be filled with calcite due to terrestrial weathering. In the case of the Martian meteorites, it is also possible that in situ weathering occurred before the fragment was ejected from Mars—this, of course, in part depends on the availability of surface water and the ancient Martian climate. Studies of pre-eruptive water content of the Martian basalts have suggested possible ranges between a few hundred ppm H₂O (Mysen et al. 1998) to nearly 2 wt% (Dann et al. 2001), although these results have been thought to be problematic (see Herd et al. 2005 for discussion). Interestingly, secondary mineral inclusions of calcite and gypsum have been found in the shergottite EET A79001, and Gooding et al. (1987) suggest that these minerals formed while the host material was on Mars. Likewise, shock effects relating to collisions

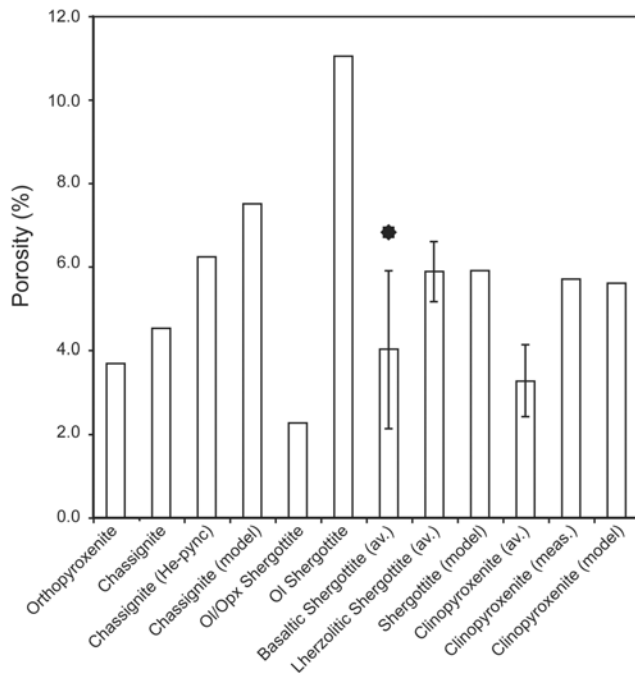


Fig. 5. Summary bar graph of available porosity data for the Martian meteorites. Data derive from this study (as determined by both methods), Britt and Consolmagno (2003) (“model” porosity data for chassignite, shergottite, and clinopyroxenite groups and a single value for clinopyroxenite calculated from bulk and grain density determinations), and McCausland and Flemming (2006) (basaltic shergottite, also calculated from density data; indicated by a filled star). “av.” is the average value for members of a particular group, with standard deviation around the mean value shown by error bars.

and/or the ejection process will have an effect on porosity. With respect to the ordinary chondrites studied by Consolmagno et al. (1998), the porosity was found, in general, to decrease with both increasing terrestrial residency time and with increasing levels of shock processing. The trends, however, are far from being linear and/or universal. Pesonen et al. (1997) find, for example, that the porosity of L chondrites decreases reasonably consistently with increasing shock index. The H chondrites, on the other hand, show no apparent tendency for the porosity to decrease with increasing shock index. Consolmagno et al. (1998) appropriately comment that “clearly, shock can reduce the porosity of some meteorites, but there is no way to predict a priori which meteorites have or have not had their porosity reduced in this manner.” However, Straight and Consolmagno (2004) show that while there is not a consistent pattern between the amount of porosity and the type of meteorite, there are hints that different types of meteorites cluster. And while there are insufficient samples to make statistically significant conclusions from these data, their observations led them to conclude that micro-crack porosity observed in the meteorites may have its origin in a process common to all meteoritic material, such as impact and ejection of the meteorite.

Unfortunately, if this is the case, then the observed meteorite (micro-crack) porosity may tell us little about the early history of the Martian meteorites (Straight and Consolmagno 2004).

Wilkison and Robinson (2000b) similarly found a lack of correlation between meteorite group and porosity, but they did observe a strong correlation between porosity and bulk density for the ordinary chondrites. This is suggestive of the possibility that it is the porosity that “controls” the bulk density within at least the chondrite groups. Flynn (2004) has further considered the effect of porosity on mechanical strength, and identifies an “atmospheric filter,” arguing that meteorites with high porosity are likely to preferentially undergo fragmentation during atmospheric ablation. The high-porosity Tagish Lake meteorite (Hildebrand et al. 2006) with $\phi \sim 40\%$, for example, produced an extensive strewn field composed of many thousands of fragments, indicative of a very weak parent body. This being said, Consolmagno et al. (1998) found no correlation between porosity and sample size (for a mass range varying from 0.002 to 2 kg). In a similar fashion to the Martian meteorites, the literature concerning the porosity and structural characteristics of the various stony achondrite meteorite groups (e.g., the HED, aubrite, and ureilite meteorite groups) is scarce and no detailed studies have been published.

At the present time, and in spite of the greatly increased data set presented in this study, there is still only a limited base from which to draw any clear-cut conclusions concerning the porosity of Martian meteorites. Table 1 indicates, however, that for the shergottite group, we find a porosity range of $1.94 \leq \phi (\%) \leq 11.04$. For the nakhlite group, we find a range of $1.92 \leq \phi (\%) \leq 4.48$. The single orthopyroxenite ALH 84001 meteorite has a measured porosity of 3.69%. From SEM/IA measurements of two thin sectioned fragments and the study of a 2.58 g bulk sample, we find $3.49 \leq \phi (\%) \leq 6.23$ for the dunite group meteorite Chassigny.

In a comparison of these new results with the existing data for the Martian meteorite groups (Fig. 5), we find, for example, that the model porosity value estimated on the basis of modal mineralogy for the basaltic shergottite group (5.9%) (Britt and Consolmagno 2003) lies toward the upper end of our determinations. However, if this model porosity value is taken for the shergottite group as a whole, we find a good match with our results. McCausland and Flemming (2006) also present a preliminary porosity value for the basaltic shergottite Zagami and quote a value of 6.8%, calculated from bulk and grain density measurements. With respect to the dunite and clinopyroxenite groups, the published model porosity data (Britt and Consolmagno 2003) are systematically higher than that determined in this study via either method. While Britt and Consolmagno (2003) suggest that SEM/IA may systematically underestimate porosity compared to bulk sample methods, it could be argued that the

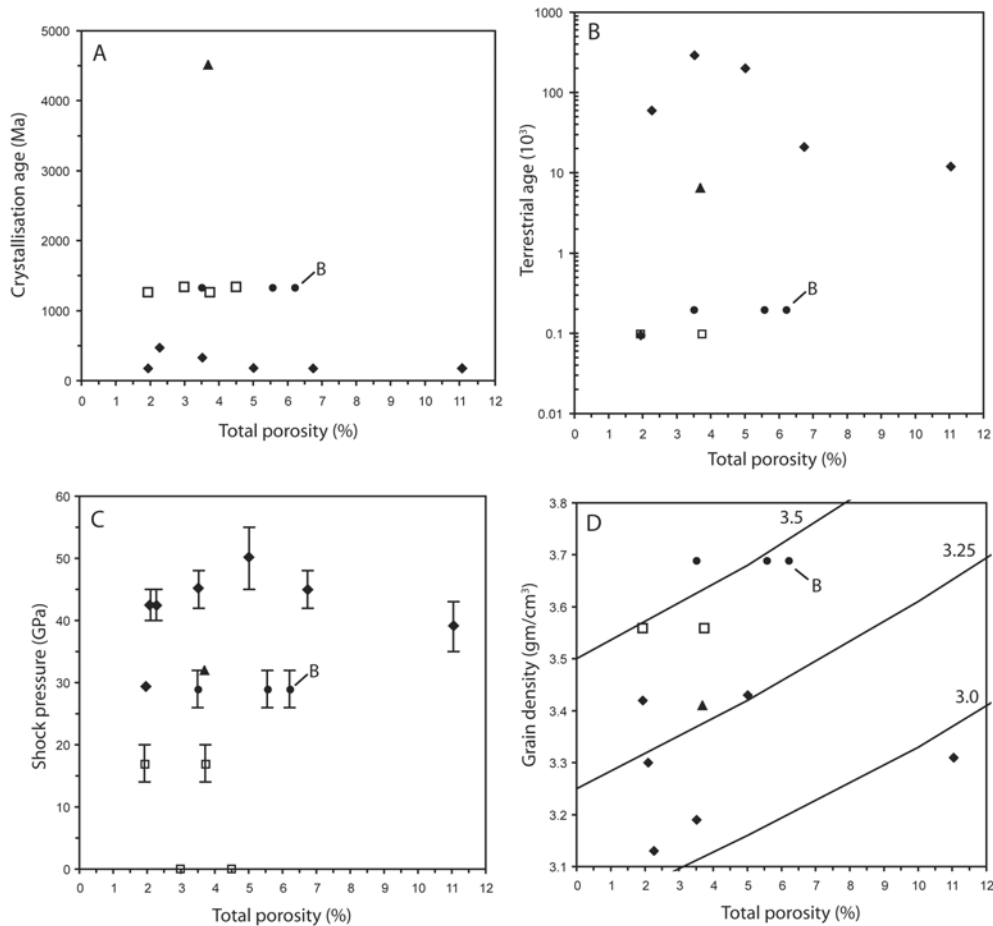


Fig. 6. a) Crystallization age versus ϕ comparison plots. The porosities are from this study, while the crystallization age data are from the Mars Meteorite Compendium (Meyer 2006). The dunite (Chassigny specimen) value labeled “B” is a bulk density porosity measurement—all other values are SEM/IA determined. b) Terrestrial residency versus ϕ . The terrestrial age data are from the Mars Meteorite Compendium (Meyer 2006). The shergottite (Zagami) and clinopyroxenite (Nakhla P7635) data points overlap each other. c) Maximum shock pressure versus ϕ . The shock pressures are taken from Fritz et al. (2005), with the exception of that for the MIL 03346 samples, which derives from Chennaoui et al. (2006). The porosity for the shergottite (Sayh al Uhaymir 005) is from Consolmagno and Strait (2002). d) Grain density versus ϕ . The grain density for Shergottite (Sayh al Uhaymir 005) is from Consolmagno and Strait (2002). Grain densities for orthopyroxenite and shergottites (ALHA77005, EETA79001, and QUE 94201) are from Lodders (1998). The curved lines are labeled according to bulk density (ρ_b) and determined according to ϕ (%) = $100 \times (1 - \rho_b/\rho_g)$. Sample key for all plots is as for Fig. 3.

“model” porosity as determined from the basis of expected grain densities given meteorite modal mineralogy is also inappropriate. However, it is highly probable that any difference relates to meteorite heterogeneity, a problem that is enhanced through the small sample size that is typical for loaned meteorite material. We therefore suggest caution in using and interpreting both our data and that determined from bulk methods until additional studies provide further confirmation of the reliability of either methods of porosity and density determination.

Leaving the above issue aside and using data gathered from across the literature, we plot the estimated crystallization age against porosity for our measured samples in Fig. 6a. While we have studied meteorites from a number of the proposed ejection epochs, the majority of our samples are derived from Martian magma that crystallized some 200

to 500 million years ago. There appears to be no obvious correlation between crystallization age and porosity, although the data is sparse for crystallization ages greater than 1 Gyr. The orthopyroxenite has the longest on-Mars residency time of all the Martian meteorites studied to date, and while carbonate infilling of porosity is deduced for this meteorite (produced while its parent mass resided on Mars), it was apparently not excessive weathering that occurred while on the planet. Again, using data gleaned from the literature, we plot the estimated terrestrial residency time against porosity in Fig. 6b. No obvious trends are apparent. There is no specific tendency, for example, for the porosity to be lower in those meteorites with longer terrestrial residency times.

From the data provided in Table 1 of Fritz et al. (2005), we plot in Fig. 6c the variation of the maximum shock pressure experienced against porosity. No clear trend emerges

from this figure. For shock pressures between ~40–50 GPa, the porosity is found to vary from between 2 and 11%. At these high shock pressures, we are perhaps seeing a “null” overall effect on the porosity, with the shock opening as many new cracks and fissures as primary ones that are closed. At these high pressures, however, the effects of permanent phase changes of minerals, mosaicism, and shock melt pocket formation become increasingly important (Thoma et al. 2005; Fritz et al. 2005). We also note that the conversion of melt phases to glass is likely to result in localized weathering rates that are higher than those experienced by surrounding phases with a concomitant increase in porosity with terrestrial age. In contrast, the porosity might be reduced by the conversion of plagioclase to maskelynite (diaplectic plagioclase glass) by shock. While in most cases maskelynite has retained the elongated lath forms of the original plagioclase crystals and is colorless, the maskelynite in shergottite LEW 88516 is observed to occur in shapes that suggest void-filling between cumulus grains (Harvey et al. 1993). In addition, according to Mikouchi et al. (1998), maskelynite in Zagami is not diaplectic glass, but rather “melted” birefringent plagioclase. Below a maximum shock pressure of ~35 GPa, Fig. 6c indicates a possible very slight correlation in which the porosity decreases with decreasing shock pressure. This latter observation is the exact reverse of the trend found by Pesonen et al. (1997) for the ordinary chondrites, but it might be an indication that the amount of microporosity increases with increasing shock experienced. Future analysis of only slightly shocked Martian meteorites (such as clinopyroxenites: Lafayette and Yamato-000593) might provide further insight into this possibility. However, in general it is clear that the clinopyroxenites are less shocked than the other Martian meteorite groups.

The variation of grain density with porosity is shown in Fig. 6d. Here we see a reasonably distinct separation of the Martian meteorite groups, with the shergottites having smaller bulk and grain densities than the dunites. This result is as expected since clinopyroxenite and dunite are cumulate rocks with more dense phases (e.g., olivine) than the shergottites, which are the equivalent of basaltic lavas. Furthermore, the grain density of any meteorite is determined by the very chemical and mineralogical properties that define each class, and so should be the same (or similar) for each class member. In terms of grain density, our values compare quite favorably to the data set of the theoretical bulk densities predicted by Lodders (1998) in terms of main Martian meteorite grouping. For example, basaltic shergottite, clinopyroxenite and dunite all show that theoretical density derived from whole-rock compositional data is typically 0.1–0.2 g/cm⁻³ lower than our calculated grain densities, highlighting again the importance of porosity in their make-up. Unfortunately, not all samples included herein were part of the Lodders (1998) study, thus precluding a detailed comparison.

CONCLUSIONS

From our sample data presented in Table 1, we note good agreement between porosity measured at 100× and 300× magnification for the shergottite meteorite group, while the other meteorite types (which represent ultramafic cumulate rocks) show less clear trends. Porosity as determined by both methods is found to relate to a number of complex factors, such as primary crystallization, weathering (alteration), shock effects, terrestrial residency, and the environment where the meteorite was recovered. Despite the increased data set relating to both porosity and density values, when plotted against a number of different variables (such as crystallization age or ejection date), the meteorites clearly indicate that what one might expect in the form of correlations is not actually seen; surprisingly, there is no clear trend of increasing shock effects and reduction in porosity. It is clear that we need to continue to collect further data on these Martian meteorites to see if any of the preliminary trends discerned are valid.

Acknowledgments—Financial support for this research derives from NSERC Discovery Grants to I. M. C. and M. B., and an NSERC undergraduate student research award to W. N. We thank Campion College and the Provincial Government of Saskatchewan for providing funding for W. N. under the Centennial Student Employment Program. We extend our thanks to Dr. C. Herd (University of Alberta), Dr. R. Herd (Geological Survey of Canada, Ottawa), and Dr. C. L. Smith (Natural History Museum, London) for the loan of meteorite samples. Our gratitude is also extended to the ANSMET loan request committee for the ALH, ALHA, EETA, QUE, and MIL samples used in this study. We further thank Dr. J. K. Russell and Dr. L. Kennedy for access to the He pycnometry facilities at the Centre for the Experimental Study of the Lithosphere (CESL), Department of Earth and Ocean Sciences, University of British Columbia, and Dr. A. Rust and N. Peterson for their time in training us in the use of these facilities. This manuscript has benefited significantly from the insightful and constructive reviews by G. Consolmagno, M. Strait, and P. McCausland, to whom we are very grateful.

Editorial Handling—Dr. Allan Treiman

REFERENCES

- Beech M. and Coulson I. 2005. The porosity of Martian meteorite Dar al Gani 476 (abstract #SE0541). 5th Canadian Space Exploration Workshop. CD-ROM.
- Bridges J. C. and Warren P. H. 2006. The SNC meteorites: Basaltic igneous processes on Mars. *Journal of the Geological Society* 163:229–251.
- Bridges J. C., Catling D. C., Saxton J. M., Swindle T. D., Lyon I. C., and Grady M. M. 2001. Alteration assemblages in Martian meteorites: Implications for near-surface processes. *Space Science Review* 96:365–392.

- Britt D. T. and Consolmagno G. J. 2003. Stony meteorite porosities and densities: A review of the data through 2001. *Meteoritics & Planetary Science* 38:1161–80.
- Chennaoui A. H., Jambon A., and Boudouma O. 2006. A cathodoluminescence study of cristobalite and K-feldspar in the nakhlite MIL 03346 (abstract). *Meteoritics & Planetary Science* 41:A37.
- Clayton R. N. and Mayeda T. K. 1996. Oxygen isotope studies of achondrites. *Geochimica et Cosmochimica Acta* 60:1999–2017.
- Consolmagno G. J. and Britt D. T. 1998. The density and porosity of meteorites from the Vatican collection. *Meteoritics & Planetary Science* 33:1231–1241.
- Consolmagno G. J. and Strait M. M. 2002. The density and porosity of Martian meteorites (abstract #32-4). Geological Society of America Meeting Abstracts with Programs.
- Consolmagno G. J., Britt D. T., and Stoll C. P. 1998. The porosity of ordinary chondrites: Models and interpretations. *Meteoritics & Planetary Science* 33:1221–1229.
- Consolmagno G. J., Macke R. J., Rochette P., Britt D. T., and Gattacceca J. 2006. Density, magnetic susceptibility, and the characterization of ordinary chondrite falls and showers. *Meteoritics & Planetary Science* 41:331–342.
- Corrigan C. M., Zolensky M. E., Dahl J., Long M., Weir J., Sapp C., and Burkett P. J. 1997. The porosity and permeability of chondritic meteorites and interplanetary dust particles. *Meteoritics & Planetary Science* 32:509–515.
- Crozaz G. and Wadhwa M. 2001. The terrestrial alteration of Saharan shergottites Dar al Gani 476 and 489: A case study of weathering in a hot desert environment. *Geochimica et Cosmochimica Acta* 65:971–78.
- Dann J. C., Holzheid A. H., Grove T. L., and McSween H. Y. Jr. 2001. Phase equilibria of the Shergotty meteorite: Constraints on pre-eruptive water contents of Martian magmas and fractional crystallization under hydrous conditions. *Meteoritics & Planetary Science* 36:793–806.
- Eugster O., Busemann H., Lorenzetti S., and Terribilini D. 2002. Ejection ages from ^{81}Kr - ^{83}Kr dating and pre-atmospheric sizes of Martian meteorites. *Meteoritics & Planetary Science* 37:1345–1360.
- Flynn G. J. 2004. Physical properties of meteorites and interplanetary dust particles: Clues to the properties of the meteors and their parent bodies. *Earth, Moon, and Planets* 95:361–374.
- Fritz J., Artemieva N., and Creshake A. 2005. Ejection of Martian meteorites. *Meteoritics & Planetary Science* 40:1393–1411.
- Gooding J. L., Wentworth S. J., and Zolensky M. E. 1987. Martian (?) calcite and gypsum in shergottite EETA79001 (abstract). 18th Lunar and Planetary Science Conference. pp. 345–346.
- Goodrich C. A. 2002. Olivine-phyric Martian basalts: A new type of shergottite. *Meteoritics & Planetary Science* 37:B31–B34.
- Harvey R. P., Wadhwa M., McSween H. Y. Jr., and Crozaz G. 1993. Petrography, mineral chemistry, and petrogenesis of Antarctic shergottite LEW 88516. *Geochimica et Cosmochimica Acta* 57:4769–4783.
- Head J. N., Melosh H. J., and Ivanov B. A. 2002. Martian meteorite launch: High-speed ejecta from small craters. *Science* 298:1752–1756.
- Herd C. D. K., Treiman A. H., McKay G. A., and Shearer C. K. 2005. Light lithophile elements in Martian basalts: Evaluating the evidence for magnetic water degassing. *Geochimica et Cosmochimica Acta* 69:2431–2440.
- Herkenhoff K. E., Squyres S. W., Arvidson R., Bass D. S., Bell J. F. III, Bertelsen P., Cabrol N. A., Gaddis L., Hayes A. G., Hviid S. F., Johnson J. R., Kinch K. M., Madsen M. B., Maki J. N., McLennan S. M., McSween H. Y. Jr., Rice J. W. Jr., Sims M., Smith P. H., Soderblom L. A., Spanovich N., Sullivan R., and Wang A. 2004. Textures of the soils and rocks at Gusev crater from Spirit's microscopic imager. *Science* 305:824–826.
- Hildebrand A. R., McCausland P. J. A., Brown P. G., Longstaffe F. J., Russell S. D. J., Tagliaferri E., Wacker J. F., and Mazur M. J. 2006. The fall and recovery of the Tagish Lake meteorite. *Meteoritics & Planetary Science* 41:407–431.
- Lin Y., Guan Y., Wang D., Makoto K., and Leshin L. A. 2005. Petrogenesis of the new Iherzolitic shergottite Grove Mountains 99027: Constraints of petrography, mineral chemistry, and rare earth elements. *Meteoritics & Planetary Science* 40:1599–1619.
- Lodders K. A. 1998. Survey of shergottite, nakhlite, and chassigny meteorites whole-rock compositions. *Meteoritics & Planetary Science* 33:A183–190.
- McSween H. Y. Jr. 1994. What we have learned about Mars from SNC meteorites. *Meteoritics* 29:757–779.
- McSween H. Y. Jr. and Treiman A. H. 1998. Martian meteorites. In *Planetary materials*, edited by Papike J. J. Reviews in Mineralogy, vol. 36. Washington, D.C.: Mineralogical Society of America. pp. 6–1–6–53.
- Meyer C. 2006. The Mars Meteorite Compendium. JSC #27672 Revision C. Houston, Texas: Astromaterials Research & Exploration Science (ARES). <http://www-curator.jsc.nasa.gov/antmet/mmc/index.cfm>.
- Mikouchi T., Miyamoto M., and McKay G. A. 1998. Mineralogy of Antarctic basaltic shergottite Queen Alexandra Range 94201: Similarities to Elephant Moraine A79001 (lithology B) Martian meteorite. *Meteoritics & Planetary Science* 33:181–189.
- McCausland P. J. A. and Flemming R. L. 2006. Preliminary bulk and grain density measurements of Martian, HED and other achondrites (abstract #1574). 37th Lunar and Planetary Science Conference. CD-ROM.
- Mysen B. O., Virgo D., Popp R. K., and Bertka C. M. 1998. The role of H_2O in Martian magmatic systems. *American Mineralogist* 83:942–946.
- Pesonen L. J., Kuoppamäki K., Timonen J., Hartikainen J., Terho M., and Hartikainen K. 1997. On the porosity of L and H chondrites (abstract #1684). 28th Lunar and Planetary Science Conference. CD-ROM.
- Rust A. C., Russell J. K., and Knight R. J. 1999. Dielectric constant as a predictor of porosity in dry volcanic rocks. *Journal of Volcanology and Geothermal Research* 91:79–96.
- Squyres S. W., Grotzinger J. P., Arvidson R. E., Bell J. F. III, Calvin W., Christensen P. R., Clark B. C., Crisp J. A., Farrand W. H., Herkenhoff K. E., Johnson J. R., Klingelhöfer G., Knoll A. H., McLennan S. M., McSween H. Y. Jr., Morris R. V., Rice J. W. Jr., Rieder R., and Soderblom L. A. 2004. In situ evidence for an ancient aqueous environment at Meridiani Planum, Mars. *Science* 306:1709–1714.
- Strait M. M. and Consolmagno G. J. 2001. Microscale variations in porosity across a meteorite (abstract). *Meteoritics & Planetary Science* 36:A199.
- Strait M. M. and Consolmagno G. J. 2002. The nature and origin of meteorite porosity: Evidence from thin section analysis (abstract). *Meteoritics & Planetary Science* 37:A137.
- Strait M. M. and Consolmagno G. J. 2003. Porosity of basaltic materials: Terrestrial and meteoritic samples (abstract). *Meteoritics & Planetary Science* 38:A106.
- Strait M. M. and Consolmagno G. J. 2004. Microcrack porosity in meteorites: Clues to early history (abstract #0998)? *Eos* 85:33A.
- Strait M. M. and Consolmagno G. J. 2005. Validation of methods used to determine microcrack porosity in meteorites (abstract #2073). 36th Lunar and Planetary Science Conference. CD-ROM.
- Taylor L. A., Nazarov M. A., Shearer C. K., McSween H. Y. Jr., Cahill J., Neal C. R., Ivanova M. A., Barsukova L. D., Lentz

- R. C., Clayton R. N., and Mayeda T. K. 2002. Martian meteorite Dhofar 019: A new shergottite. *Meteoritics & Planetary Science* 37:1107–1128.
- Thoma K., Hornemann U., Sauer M., and Schneider E. 2005. Shock waves—Phenomenology, experimental, and numerical simulation. *Meteoritics & Planetary Science* 40:1283–1298.
- Wilkison S. L. and Robinson M. S. 1999. Bulk density measurements of meteorites (abstract #1929). 30th Lunar and Planetary Science Conference. CD-ROM.
- Wilkison S. L. and Robinson M. S. 2000a. Some bulk density measurements of ordinary chondrites (abstract #1939). 31st Lunar and Planetary Science Conference. CD-ROM.
- Wilkison S. L. and Robinson M. S. 2000b. Bulk density of ordinary chondrite meteorites and implications for asteroidal internal structure. *Meteoritics & Planetary Science* 35:1203–1213.
- Wilkison S. L., McCoy T. J., McCamant J. E., Robinson M. S., and Britt D. T. 2003. Porosity and density of ordinary chondrites: Clues to the formation of friable and porous ordinary chondrites. *Meteoritics & Planetary Science* 38:1533–1546.
- Yomogida K. and Matsui T. 1983. Physical properties of ordinary chondrites. *Journal of Geophysical Research* 88:9513–9533.
-